



## Muscovy duck reovirus p10.8 protein induces ER stress and apoptosis through the Bip/IRE1/XBP1 pathway



Quanxi Wang<sup>a,b,\*</sup>, Mengxi Liu<sup>a,b</sup>, Yuan Chen<sup>a,b</sup>, Lihui Xu<sup>a</sup>, Baocheng Wu<sup>a,b</sup>, Yijian Wu<sup>a,b</sup>, Yifan Huang<sup>a,b</sup>, Wei-Ru Huang<sup>c,d</sup>, Hung-Jen Liu<sup>c,d,e,f,g,\*</sup>

<sup>a</sup> College of Animal Science, Fujian Agriculture and Forestry University, Fuzhou, 350002, PR China

<sup>b</sup> Fujian Key Laboratory of Traditional Chinese Veterinary Medicine and Animal Health (Fujian Agriculture and Forestry University), Fuzhou, Fujian, 350002, PR China

<sup>c</sup> Institute of Molecular Biology, National Chung Hsing University, Taichung 402, Taiwan

<sup>d</sup> The iEGG and Animal Biotechnology Center, National Chung Hsing University, Taichung 402, Taiwan

<sup>e</sup> Rong Hsing Research Center for Translational Medicine, National Chung Hsing University, Taichung 402, Taiwan

<sup>f</sup> Ph.D Program in translational Medicine, National Chung Hsing University, Taichung 402, Taiwan

<sup>g</sup> Department of Life Sciences, National Chung Hsing University, Taichung 402, Taiwan

### ARTICLE INFO

#### Keywords:

MDRV  
p10.8 protein  
ER stress  
Apoptosis  
Bip  
IRE1  
XBP1  
Caspase 3

### ABSTRACT

In the present study, the mechanisms underlying Muscovy duck reovirus (MDRV) p10.8 protein-induced ER stress and apoptosis in DF-1 cells and Muscovy duckling hepatic tissues were explored. On the fifth day post-infection, an increase in the mRNA levels of binding immunoglobulin protein (Bip) and X-box binding protein (XBP1), activation of XBP1/s, and an increase in percentage of apoptotic cells were observed in Muscovy duckling livers. The use of ER stress inducer Tunicamycin and ER stress inhibitor Tauroursodeoxycholic acid demonstrated that MDRV induces apoptosis via ER stress, leading to apoptosis. The use of Tunicamycin increased viral protein synthesis while Tauroursodeoxycholic acid reduced viral protein synthesis, suggesting that MDRV induces ER stress benefiting virus replication. The MDRV p10.8 is the major protein to induce ER stress and apoptosis. We found that p10.8 promotes the conversion of XBP1/u to XBP1/s and expands ER diameter, and increases the percentages of apoptotic cells in DF-1 and duckling liver tissues. To investigate the mechanism underlying the MDRV p10.8-induced ER stress and apoptosis, Western blot, siRNA, and co-immunoprecipitation (Co-IP) assays were performed. We found that the MDRV p10.8 protein up-regulates Bip, p-IRE1, XBP1s, and cleaved-caspase 3. Co-IP results reveal that the MDRV p10.8 protein disassociates the Bip/IRE1 complex. Inhibition of IRE1 by 4-methyl umbelliferone 8-carbaldehyde (4u8c) dramatically reversed the MDRV p10.8-modulated increase in levels of XBP1s and cleaved-caspase 3. Knockdown of XBP1 by siRNA reversed the increased level of p10.8-modulated cleaved-caspase 3. The present study provides mechanistic insights into the MDRV p10.8 protein induces ER stress, resulting in apoptosis via the Bip/IRE1/XBP1 pathway in DF-1 cells and duckling livers.

### 1. Introduction

The infection of ducks with reovirus was first reported in 1950 (Kaschula, 1950), however, Muscovy duck reovirus (MDRV) was first isolated in 1972 (Gaudry et al., 1972). In China, there have been regular outbreaks of MDRV diseases since 1997, which have caused serious economic losses to the duck farming industry (Wu et al., 2001; Wang et al., 2015). Recently, the YB strain of MDRV causes extensive “white necrosis” in the liver and spleen of ducklings with high mortality (Wang et al., 2015; Wang et al., 2017b). In our earlier report, we found that

MDRV strongly induced apoptosis in duckling hepatic cells, which were regulated by multiple signaling pathways, such as Fas and NF- $\kappa$ B pathway (Wang et al., 2017a). Our team also found that MDRV infection inhibited the cholesterol efflux and fatty acid degradation in hepatic cells, leading to the accumulation of fatty acids and cholesterol in the liver cells. Hepatic necrosis caused by MDRV is related to an abnormality of fatty acid metabolism (Wang et al., 2017b). Furthermore, we found that the MDRV p10.8 protein induces ER stress leading to cell cycle arrest at G1 phase and apoptosis through the PERK/eIF2 $\alpha$  pathway in duckling livers and DF-1 cells (Wang et al., 2018). The

\* Corresponding author at: Institute of Molecular Biology, National Chung Hsing University, Taichung 402, Taiwan.

\*\* Corresponding author at: Fujian Agriculture and Forestry University, Fuzhou, 350002, PR China.

E-mail addresses: [wqx608@fafu.edu.cn](mailto:wqx608@fafu.edu.cn) (Q. Wang), [hjliu5257@nchu.edu.tw](mailto:hjliu5257@nchu.edu.tw) (H.-J. Liu).

sequence of the MDRV S-segment gene is significantly different from other avian reovirus (ARV) S-segment genes. In particular, the homology of the MDRV p10.8- and ARV p10-encoding genes is only 21.90% (Cai et al., 2015). Furthermore, MDRV lacks the p17 protein. An earlier report indicated that the ARV p10 protein induces syncytium formation by utilizing RhoA and Rac1-dependent signaling pathways (Liu et al., 2008).

The signaling pathways of apoptosis include the death receptor pathway, mitochondrial pathway, and endoplasmic reticulum pathway. In recent years, the endoplasmic reticulum pathway of apoptosis induction has caused concerns to researchers (Hu et al., 2017; Zhao et al., 2017). Viral infection may induce endoplasmic reticulum (ER) stress, and higher levels of prolonged ER stress would result in apoptosis by activating CHOP (Gu et al., 2017) and c-Jun N-terminal kinase (JNK) (Zhang et al., 2016) or caspases 3 and 12 (Cao et al., 2014). Inositol-requiring enzyme 1 (IRE1) is an important ER transmembrane sensor that activates the unfolded protein reaction (UPR) to maintain ER function (Amin-Wetzel et al., 2017). Under normal physiological cellular conditions, IRE1 forms a complex with binding immunoglobulin protein (Bip/GRP78). When host cells are infected by viruses, which lead to an increase in the levels of defective folded or unfolded proteins in ER, leading to Bip/IRE1 dissociation. Subsequently, IRE1 is phosphorylated and activated. The phosphorylated form of IRE1 (p-IRE1) cuts off the 26bp intron of X-box binding protein unspliced (XBP1u) mRNA to form XBP1s (spliced) (Taylor and Dillin, 2013). XBP1s then targets the nucleus and upregulates caspase 3 and CHOP to induce apoptosis (Jiang et al., 2017).

Several viruses are known to induce apoptosis through ER stress such as HIV-1 gp120 induces type-1 programmed cell death through ER stress, employing the IRE1 $\alpha$ , JNK, and activator protein (AP-1) pathways (Shah et al., 2016). The Japanese encephalitis virus induces apoptosis through the IRE1/JNK pathway of ER stress response in BHK-21 cells (Huang et al., 2016). Recently, Guo reported that the MDRV p10.8 protein is localized to the nucleus (Guo et al., 2014). Previous studies suggested that MDRV induces apoptosis (Geng et al., 2009; Wang et al. 2017a; Wang et al., 2018). In our previous report, we demonstrated that MDRV induces apoptosis in liver and DF-1 cells, and the MDRV p10.8 protein induced cell cycle arrest at G1 phase and apoptosis via PERK/eIF2 $\alpha$  pathway (Wang et al., 2018). However, it is still unclear whether MDRV induced apoptosis is related to Bip/IRE1/XBP1 pathway. Liver is the major target organ during MDRV infection. To date, there is still no duck-derived cell line, and DF-1 has become a model cell line for many avian virus studies. Therefore, we firstly investigated the relationship of ER stress and apoptosis in duckling hepatic cells- and DF-1 cells-infected with MDRV. In the present study, we aimed to explore that the MDRV p10.8 induces apoptosis by inducing ER stress through the Bip/IRE1/XBP1 pathway in DF-1 cells and duckling liver tissues.

## 2. Materials and methods

### 2.1. Ethics statement

All ducks used in the experimental procedures were treated in accordance with the Regulations for the Administration of Affairs Concerning Experimental Animals approved by the State Council of China. The animal protocols used in this study were approved by the Research Ethics Committee of College of Animal Science, Fujian Agriculture and Forestry University, China.

### 2.2. Viruses, cell culture, and plasmid transfection

MDRV strain YB was propagated in Muscovy duck embryo fibroblasts (MDEFs), which were cultured in RPMI 1640 medium (Hyclone, Logan, USA) supplemented with 2% fetal bovine serum (FBS; Hyclone, Logan, USA), as previously described (Wang et al., 2017a). Since no

duck-derived cell line is available, we used the chicken embryo fibroblast 1 (DF-1) cell line in this study to investigate that the MDRV p10.8 induces apoptosis by inducing ER stress through the Bip/IRE1/XBP1 pathway. The DF-1 cells was grown in Dulbecco's modified eagle medium (DMEM; Hyclone, Logan, USA) supplemented with 10% FBS. Cells that exhibited 70% confluence were transfected with plasmids using Lipofectamine 2000 reagent (Promega, Wisconsin, USA).

### 2.3. Reagents, plasmids, and antibodies

The ER stress inhibitor Tauroursodeoxycholic acid (TUDCA) and ER stress inducer tunicamycin (TM) were purchased from Sigma (St. Louis, MO, USA). IRE1 inhibitor (4u8c) was purchased from Calbiochem (La Jolla, CA, USA). The Western bright MCF fluorescent kit was purchased from Advansta (CA, USA). Annexin V-FITC was purchased from Beyotime Biotechnology (Shanghai, China).

Total RNA extraction kit, cDNA synthesis kit, SYBR fluorescent quantitative polymerase chain reaction (fq-PCR) kit, and co-immunoprecipitation (Co-IP) kit were purchased from Promega (Wisconsin, USA). Mouse anti-Bip, -IRE1, -p-IRE1, -caspase 3, -cleaved-caspase 3, -CHOP antibodies and HRP labeled sheep against rabbit/mouse antibody were purchased from Cell Signaling Biotechnology (Beverly, MA, USA). Rabbit anti-p10.8, -XBP1s, and -XBP1u antibodies were prepared in our laboratory through prokaryotic expression and using immune rabbit.

### 2.4. Primers

Primers for reverse transcription (RT) and real time fluorescent quantitative polymerase chain reaction (fq-PCR) in this study were designed using Primer 6.0 software. Sequences of primers are shown in Table 1 for the analysis of mRNA expression levels of the following genes: *p10.8*, *Bip*, *IRE1*, *XBP1*, *CHOP*, *caspase 3*, and  $\beta$ -*actin* in the infected and non-infected groups. The experimental procedures for PCR, RT and real time fq-PCR, and Western blot assays were carried out according to descriptions in previous studies (Wang et al., 2015; Chen et al., 2015).

### 2.5. MDRV strain YB inoculation in five-day old Muscovy ducks

Twenty five-day-old ducklings, confirmed to be MDRV-negative by RT and real time fq-PCR and MDRV antibody-negative by ELISA, were equally divided into two groups. Treatment groups were individually infected with MDRV strain YB using a 0.2 mL (0.01 TCID<sub>50</sub> = 10<sup>-5.40</sup>) intramuscular injection; the control groups were treated with 0.2 mL of sterile saline. The ducklings were fed in isolated cages at the laboratory animal center of Fujian Agriculture and Forestry University. On the fifth day post-infection, all ducklings in the two groups were sacrificed and

**Table 1**

Primers used in this study.

Genes	Primers (5'-3')	Expected size (bp)
<i>BIP</i>	F:5'-CAGACCGATGGGAATCGGAG-3' R:5'-GCCTTCTCTCGTTCCAGGTC-3'	269
<i>Caspase3</i>	F:5'-CTGCTCCAGGCTATTACTCC-3' R:5'-GACACTCTGCGATTTACACG-3'	136
<i>CHOP</i>	F: 5'-TTCCGCTTTGTCCTCTGC-3' R: 5'-TGCTGTGAGCTGGATGAGAC-3'	288
<i>XBP1</i>	F:5'-GGAGGAGGAGAACCAGAAGC-3' R:5'-CAGAACATCCAAACCAAGC-3'	112
<i>XBP1(u/s)</i>	F:5'-GCCGCCCCGAAGCG-3' R:5'-TGAGTTCATTAATGGCCTCC-3'	139/103
<i>p10.8</i>	F: 5'-ATGGCTGATGCTTTTGAAGT-3' R:5'-CTAGTTAGATCCCGAGAGC-3'	288
$\beta$ - <i>actin</i>	F: 5'-GTGCTATGTCCGCTGGAT-3' R:5'-CCAAGAAAGATGGCTGGAAG-3'	138

their liver tissues were harvested for the detection of apoptosis and mRNA levels (Wang et al., 2015).

## 2.6. MDRV strain YB infected DF-1 cells

To verify that MDRV induces ER stress and apoptosis, DF-1 cells were cultured in 6-well plates and infected with 100  $\mu$ L of MDRV strain YB in Dulbecco's modified Eagle medium (DMEM) supplemented with 10% FBS. Normal cells were used as controls. After 24 h, the total RNA was extracted and RNA was reverse transcribed to cDNA. Alternatively, the total protein was extracted using an animal cell total protein extraction kit (purchased from Promega, Wisconsin, USA).

## 2.7. RNA extraction and RT and real time fq-PCR

RNA from the liver tissue of the two groups were extracted and cDNA were synthesized according to the manufacturer's instructions. XBP1 is the marker protein for ER stress. When the mRNA of XBP1u is cut off 26 bp from the intron, it is activated to form XBP1s, which directs the cells towards ER stress. The mRNA level of XBP1 was measured by RT and real time fq-PCR. The spliced-XBP1 levels were examined by RT-PCR. The amplified PCR product was analyzed by electrophoresis with 1.5% agarose gel. The mRNA levels of *Bip*, *XBP1*, *caspase 3*, *CHOP*, and *p10.8* were analyzed by RT and fq-PCR. The relative mRNA levels of *Bip*, *XBP1*, *caspase 3*, and *CHOP* were calculated according to the  $\Delta\Delta$ CT method. The relative mRNA levels of *p10.8* was calculated using the  $\Delta$ CT method. The PCR condition for amplification was 95 °C for 5 min; 30 cycles of 94 °C for 45 s, 50 °C for 45 s, and 72 °C for 1 min 30 s; followed by 72 °C for 8 min. The products were analyzed on 1.0% agarose gel. Real time fq-PCR was carried out as described previously (Ke et al., 2006). Real time fq-PCR consisted of 25  $\mu$ L SYBR® Premix Ex TaqTM (2 $\times$ ) (Promega, Wisconsin, USA), 5  $\mu$ L cDNA, 1  $\mu$ L forward primer (10  $\mu$ M), 1  $\mu$ L reverse primer (10  $\mu$ M), and 18  $\mu$ L RNase-free ddH<sub>2</sub>O. PCR conditions included an initial denaturation at 95 °C for 2 min followed by 40 cycles at 95 °C for 15 s, 60 °C for 30 s, and 72 °C for 30 s; finally dissociation at 65 °C for 15 s. Data were analyzed using the following formula: target gene expression =  $2^{-\Delta\Delta Ct}$  or  $2^{-\Delta Ct}$  (Nishikim, 2000);  $\beta$ -actin was used as the reference gene.

## 2.8. Detection of cell apoptosis by flow cytometry

The livers from all ducklings were cut into small pieces and homogenized with a tissue grinder. Cell suspensions were collected, filtered through a nylon mesh filter (pore size 400  $\mu$ m), stained with 500  $\mu$ L of annexin V-fluorescein isothiocyanate/propidium iodide, and analyzed by flow cytometry (BD Calibur; New Jersey, USA) to detect the percentage of apoptotic cells according to our previous study (Wang et al., 2017a).

## 2.9. Treatment of DF-1 cells with the ER stress promoter and inhibitor

In this study, the ER stress promoter TM, and the ER stress inhibitor TUDCA were used. DF-1 cells were cultured in 6-well or 12-well plates for 12 h. In the next step, we either left the medium unchanged and incubated it with MDRV for 0.5 h, or transfected with pCI-neo-p10.8 or pCI-neo, and then added the complete DMEM medium containing 10% FBS and TM, 2  $\mu$ g/mL or TUDCA, 2  $\mu$ g/mL for 24 h. The mRNA levels of *p10.8*, *Bip*, *XBP1*, *CHOP*, and *caspase 3* were detected by RT and real time fq-PCR. The spliced-XBP1 levels were examined by RT-PCR. The amplified PCR product was analyzed by electrophoresis with 1.5% agarose gel. Apoptosis was detected by flow cytometry. The ER diameter was observed using the transmission electron microscope (HT7700; Tokyo, Japan).

## 2.10. MDRV p10.8 protein induced ER stress in DF-1 cells, resulting in apoptosis

DF-1 cells were cultured in 6-wells or 12-wells for 12 h, and then the medium was discarded. DF-1 cells were transfected with pCI-neo (vector alone) and pCI-neo-p10.8 by mixing with lipofectamine 2000 for 24 h. The mRNA levels of *p10.8*, *Bip*, *XBP1*, *CHOP*, and *caspase 3* were detected by RT and real time fq-PCR. The spliced-XBP1 levels were examined by RT-PCR. The amplified PCR product was analyzed by electrophoresis with 1.5% agarose gel. Apoptosis was detected by flow cytometry. ER diameter was observed and analyzed by the transmission electron microscope (HT7700). The pCI-p10.8-transfected cells were treated with the promoter or inhibitor of ER stress and their effect on DF-1 cells were evaluated.

DF-1 cells were subcultured in 6-well or 12-well plates for 12 h and then the medium was discarded. DF-1 cells were transfected with pCI-neo and pCI-neo-p10.8 using liposome 2000 for 4 h followed with addition of DMEM medium containing 10% FBS and 2  $\mu$ g/mL TM or TUDCA for 20 h. The mRNA levels of *p10.8*, *XBP1*, *CHOP*, and *caspase 3* were detected by RT and real time fq-PCR. Percentage of apoptotic cells was detected and analyzed by flow cytometry. The ER diameter was observed under the transmission electron microscope (HT7700).

## 2.11. Suppression of IRE1 phosphorylation and XBP1 levels

The dimeric-IRE1 phosphorylate each other, and the p-IRE1 causes XBP1 to become spliced and activated. This study further investigates whether p10.8 promotes XBP1s through phosphorylation of IRE1. Five groups of DF-1 cells were prepared in a 6-well plate. The first was the control; the second was transfected with pCI-neo; the third was transfected with pCI-neo-p10.8; the fourth was treated with the IRE1 inhibitor 4u8C (final concentration 1 mmol/L); the fifth was transfected with pCI-neo-p10.8 and 4u8C was added to the cell maintenance medium. At 24 h post-transfection, cells were collected and the total proteins were extracted. Protein levels of p10.8, *Bip*, IRE1, p-IRE1, XBP1u, XBP1s, pro-caspase 3, and cleave-caspase 3 were analyzed by Western blot and analyzed by Image J software (National Institutes of Health, Maryland, USA).

XBP1-specific siRNA oligonucleotides were synthesized by Biomics Biotechnology Co., Ltd, (Nantong, China). Three XBP1-specific siRNA sequences were shown in Table 2. They were transfected into DF-1 cells, respectively, and the mRNA level of XBP1 was detected by RT and real time fq-PCR at 24 h post-transfection. The optional XBP1-specific siRNA (siXBP1 No. 3) was used to evaluate p10.8-induced DF-1 cell apoptosis. Five groups of DF-1 cells were prepared in a 6-well plate. The first was the control; the second was transfected with pCI-neo; the third was transfected with pCI-neo-p10.8; the fourth was transfected with siXBP1 and subsequently transfected for 6 h with pCI-neo-p10.8; and the fifth was transfected with siXBP1. At 24 h post-transfection, cells were collected and total mRNAs or total proteins were extracted. The mRNA levels of *p10.8*, *Bip*, *XBP1*, *caspase 3*, and *CHOP* were analyzed by RT and real time fq-PCR. The protein levels of p10.8, *Bip*, IRE1, p-IRE1, XBP1u, XBP1s, pro-caspase 3, and cleaved-caspase 3 were analyzed by

**Table 2**  
XBP1-specific siRNA sequences.

siRNA	Oligonucleotides (5'-3')	Chemical modification
XBP1-1	F 5'-GGGUUUUGAUGUUCGAAAdTdT-3' R 5'-UUUCAGAACAUCAAACCCdTdT-3'	N/A
XBP1-2	F 5'-CAGUGACUCUUCAGAUUCUdTdT-3' R 5'-AGAAUCUGAAGAGUCACUGdTdT-3'	N/A
XBP1-3 <sup>a</sup>	F 5'-GAAACAAAUUCCAUACCGAdTdT-3' R 5'-UCGGUAUGGAAUUUGUUCdTdT-3'	N/A

<sup>a</sup> The siRNA with the most significant down-regulated effect for XBP1 gene was selected and used in this study.

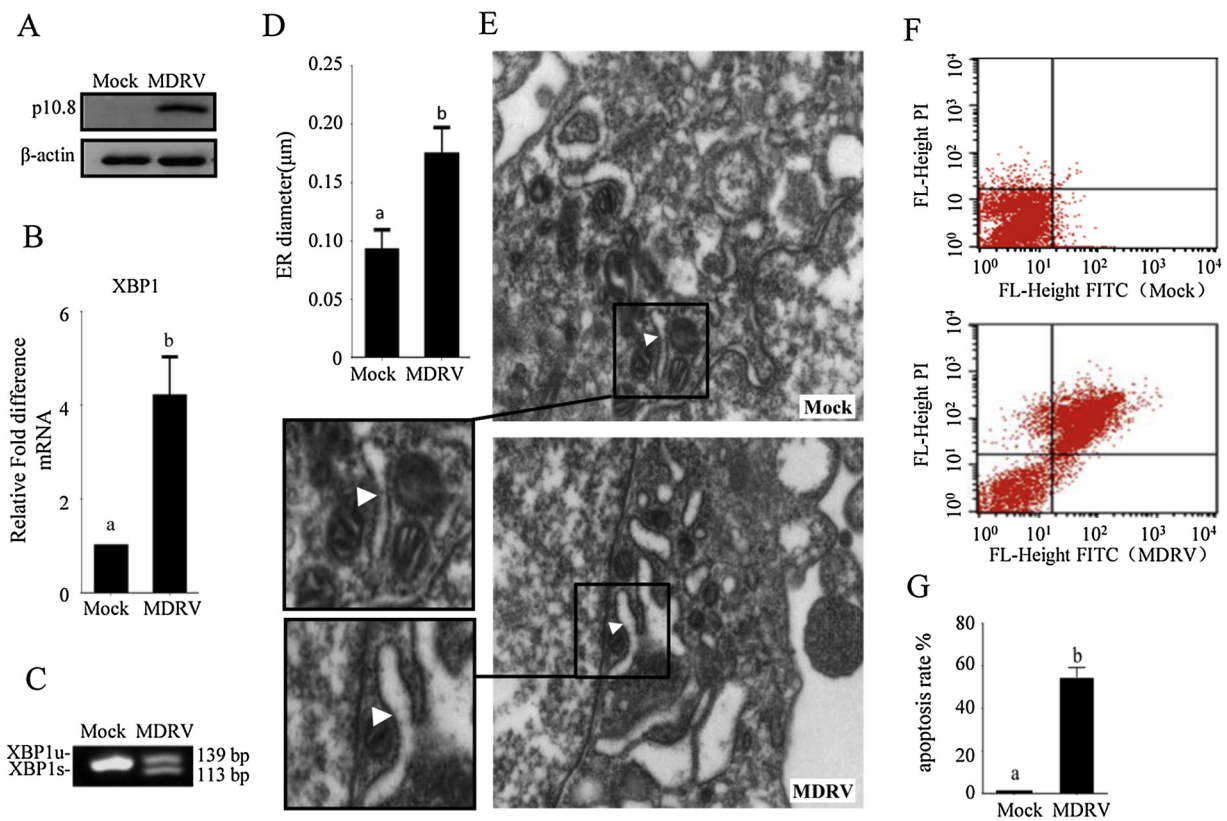


**Fig. 1.** ER stress and apoptosis induced by MDRV in duckling liver tissues. Five-day-old ducklings were infected with MDRV by a 0.2 mL (0.01 TCID<sub>50</sub> = 10<sup>-5.40</sup>) intramuscular injection. Control ducklings were treated with 0.2 mL of sterile saline. On the fifth day post-infection, all ducklings in the two groups were sacrificed and their livers were harvested. (A) The MDRV p10.8 protein was detected by Western blot assays with an anti-p10.8 protein antibody. The mRNA levels of *XBP1* (B) were detected by RT and real time fq-PCR. (C) The spliced *XBP1* level was detected by RT-PCR and PCR products were analyzed by DNA electrophoresis. (D, E) The ER of liver cells was observed by transmission electron microscope (HT7700, 8000×, arrow indicates ER), ER diameter was measured by Digital Micrograph (DM). (F, G) Apoptosis was detected by flow cytometry, and the apoptosis index was statistically analyzed (F). Statistical analysis of the proportions of cell apoptosis in MDRV-infected duckling livers (G). Significance between the treatments was determined by Student's *t*-test using SPSS software (Version 20.0). Means with different alphabets (a, b) denotes significance at *p* < 0.05. All data represents mean ± standard error (SE) of three independent experiments.

Western blot.

### 2.12. Observation by electron microscopy

The liver tissues were placed in 1 mm<sup>3</sup> of 2.5% glutaraldehyde for 2 h at 4 °C, and then, fixed in 1% osmium acid for 1 h, and subsequently embedded into group resin (epoxy). DF-1 cells were cultured in vitro with complete DMEM medium containing 10% FBS for 24 h. The medium was then discarded and 2.5% glutaraldehyde solution was added for 3 min at 4 °C. The cells were scraped using a cell scraper and centrifuged at 2000 g for 15 min. The pellet contents were treated with 2.5% glutaraldehyde for 2 h at 4 °C, and 1% osmic acid fixation for 1 h. Finally they were embedded into epoxy resin. Samples were sliced at 50–60 nm, and then double stained with 3% uranium acetate-citric acid. The ER diameters were observed and measured by HT7700 electron microscopy

### 2.13. Co-immunoprecipitation (Co-IP) assay

In conditions of ER stress, Bip dissociates from the Bip/IRE1 complex to bind with unfolded proteins. In order to study whether the MDRV p10.8 protein interact with Bip or IRE1, Co-IP assays were carried out. Immunoprecipitation was performed using the Catch and Release kit (Upstate Biotechnology, Waltham, USA), according to the manufacturers protocol. Cells were scraped from the culture plate, cracked using the cold cell lysis buffer EBC, and centrifuged for 15 min at 4 °C. The supernatant was collected and the anti-Bip or anti-IRE1

antibody was added. The suspension was shaken for 1 h at 4 °C; then, the protein A-Sepharose suspension was added for 30 min at 4 °C. A further centrifugation step was performed for 15 min at 4 °C. The protein A-Sepharose mixture was washed 5 times with NETN (900 mmol/L NaCl) and finally washed again with NETN. The liquid was heated till denaturation and then analyzed by Western blot.

### 2.14. Western blot assays

Livers or cells were collected, and were washed with 1 × PBS and lysed with lysis buffer. They were centrifuged at 13,000 g for 15 min at 4 °C. The concentration of solubilized protein was determined with the Bio-Rad Protein Assay (Bio-Rad Laboratories, USA). Equal amounts of samples were mixed with 2.5 × Lammeli loading buffer and boiled for 10 min in a water bath. The proteins were separated by SDS-PAGE and transferred to a PVDF membrane. Expression of individual proteins was determined using the corresponding primary antibody and visualized by the HRP labeled secondary antibodies. The results were detected on film (GE Healthcare Life Sciences) after membrane incubation with enhanced chemiluminescence reagent (ECL plus) (Amersham Biosciences, UK). The intensity of target proteins was calculated using Photocapt (Vilber Lourmat, France)

### 2.15. Statistical analysis

Statistical analyses were performed via Student *t*-tests or One-Way ANOVA analysis and LSD test using SPSS 20.0.

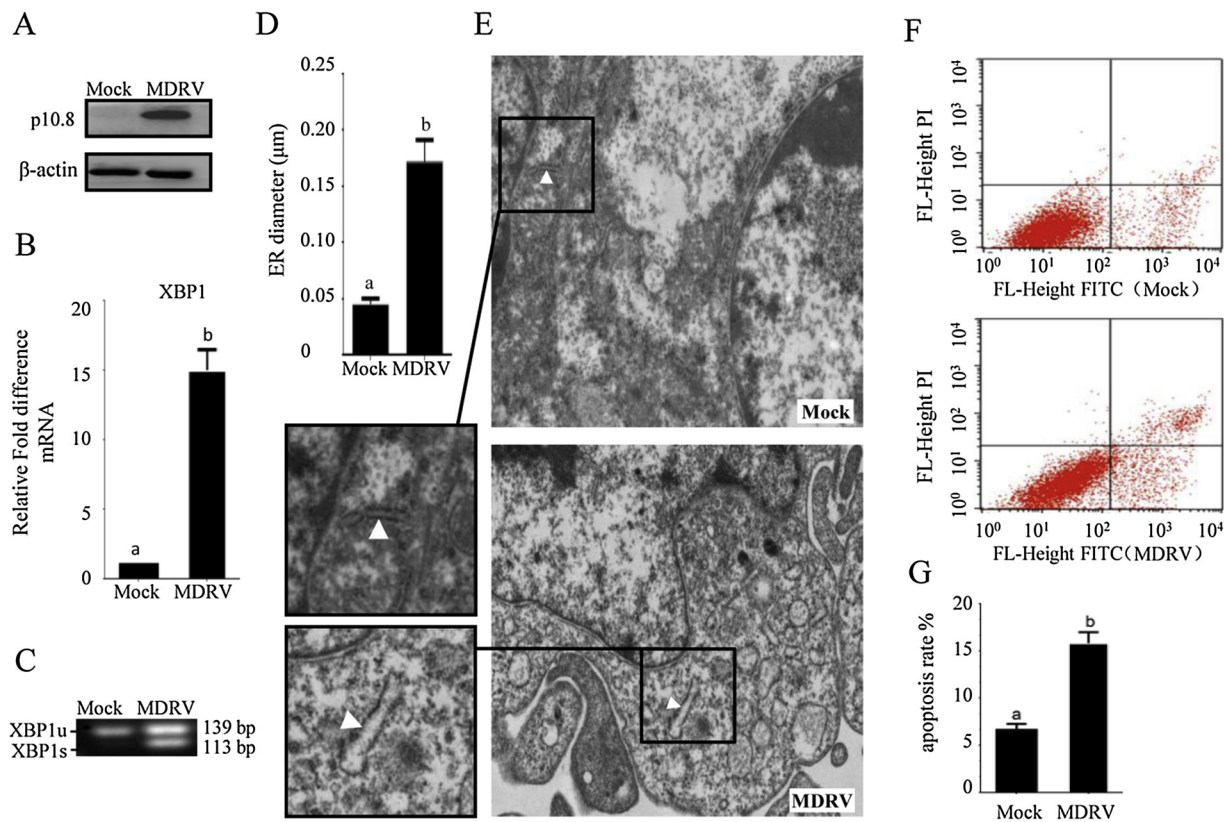


**Fig. 2.** MDRV induces ER stress and apoptosis in DF-1 cells. DF-1 cells were subcultured in 6-well plates for 24 h. One was infected with MDRV (0.2 mL; 0.01 TCID<sub>50</sub> = 10<sup>-5.40</sup>), another was treated with 0.2 mL of sterile saline. At 24 h post-infection, all cells in the two groups were collected. (A) MDRV was detected by Western blot assays with an anti-p10.8 protein antibody. The mRNA levels of *XBP1* (B) were detected by RT and real time fq-PCR. (C) The spliced *XBP1* level was detected by RT-PCR and PCR products were analyzed by DNA electrophoresis. (D, E) The ER that was in the MDRV-infected cells was examined by transmission electron microscope objection (HT7700, 8000×; arrows indicating ER), the ER diameter was measured by Digital Micrograph (DM) and was statistically analyzed. (F, G) Apoptosis was detected by flow cytometry, and the apoptosis index was statistically analyzed in DF-1 cells (F). Statistical analysis of the proportions of cell apoptosis in MDRV-infected DF-1 cells g livers (G). All data represents mean ± SE of three independent experiments. Significance between the treatments was determined by Student's *t*-test using SPSS software (Version 20.0). Means with different alphabets (a, b) denotes significance at *p* < 0.05.

### 3. Results

#### 3.1. MDRV induced ER stress and apoptosis in duckling livers

*XBP1* is an important ER stress relational protein (Jiang et al., 2017). Our results showed that on the 5th day post-infection with MDRV (Fig. 1A), the increased mRNA level of *XBP1* and the elevated conversion of *XBP1u* to *XBP1s* were seen in duckling livers (Figs. 1B and C). Electron microscopy showed that MDRV infection led to ER diameter being significantly wider in the MDRV-infected duckling liver cells than those in the mock control group (Fig. 1D-E), indicating that MDRV induces ER stress in duckling livers. Furthermore, flow cytometry results indicated that MDRV significantly induces apoptosis in duckling liver (Fig. 1F and G). Based on our findings, we suggests that MDRV infection induces ER stress and apoptosis in Muscovy duckling livers.

#### 3.2. MDRV-induced apoptosis via ER stress in DF-1 cells

DF-1 cells are a model cell line for many aspects of avian virus research (Ahronian and Lewis, 2014). The current study was also performed to investigate whether MDRV could induce ER stress and apoptosis in DF-1 cells. The expressed p10.8 protein in MDRV-infected DF-1 cells was detected (Fig. 2A). The mRNA level of *XBP1* increased significantly in MDRV-infected DF-1 cells compared with the control (Fig. 2B). Furthermore, MDRV promoted the conversion of *XBP1u* to *XBP1s* (Fig. 2C). Our results revealed that MDRV significantly causes

the ER swelling, as observed by electron microscopy (Fig. 2D and E). We found that the apoptotic rate (%) was significantly increased in MDRV-infected cells compared with that in mock control cells (Fig. 2F and G).

To further investigate whether MDRV induces apoptosis in DF-1 cells under ER stress, ER stress intensifier (TM) and inhibitor (TUDCA) were used. Our results showed that the mRNA levels of *Bip* (Fig. 3A), *XBP1* (Fig. 3B), *caspase 3* (Fig. 3C) and *CHOP* (Fig. 3D) in MDRV infected DF-1 or TM-treated cells were significantly increased compared with that in MDRV-infected DF-1 cells and the controls. The significant increase in spliced *XBP1* levels in TM-treated or MDRV-infected DF-1 cells was seen compared with that in non-treated cells and mock infection, as revealed by DNA electrophoresis (Fig. 3E; upper panel, lanes 2 and 3). The increased spliced levels of *XBP1s* by MDRV were enhanced in TM-treated DF-1 cells (Fig. 3E; lower panel, lane 4). The use of TUDCA revealed that, at 24 h post-infection, the mRNA levels of *Bip* (Fig. 3A), *XBP1* (Fig. 3B), *caspase 3* (Fig. 3C), and *CHOP* (Fig. 3D) in MDRV-infected and TM-treated DF-1 cells were significantly reduced. The mRNA levels of *XBP1* in MDRV-infected and TUDCA-treated DF-1 cells were reduced significantly compared with those of MDRV-infected DF-1 cells and the controls (Fig. 3B). The increased mRNA levels of *Bip*, *XBP1*, *caspase 3*, and *CHOP* by MDRV was reversed in TUDCA-treated DF-1 cells (Fig. 3A–D). The increased level of spliced *XBP1* by MDRV were reversed in TUDCA-treated cells (Fig. 3E; lower panel, lane 4). These results led us to further confirm that MDRV induces apoptosis via ER stress in DF-1 cells. Furthermore, we found that the use of TM increased the mRNA and protein levels of p10.8 while TUDCA reduced

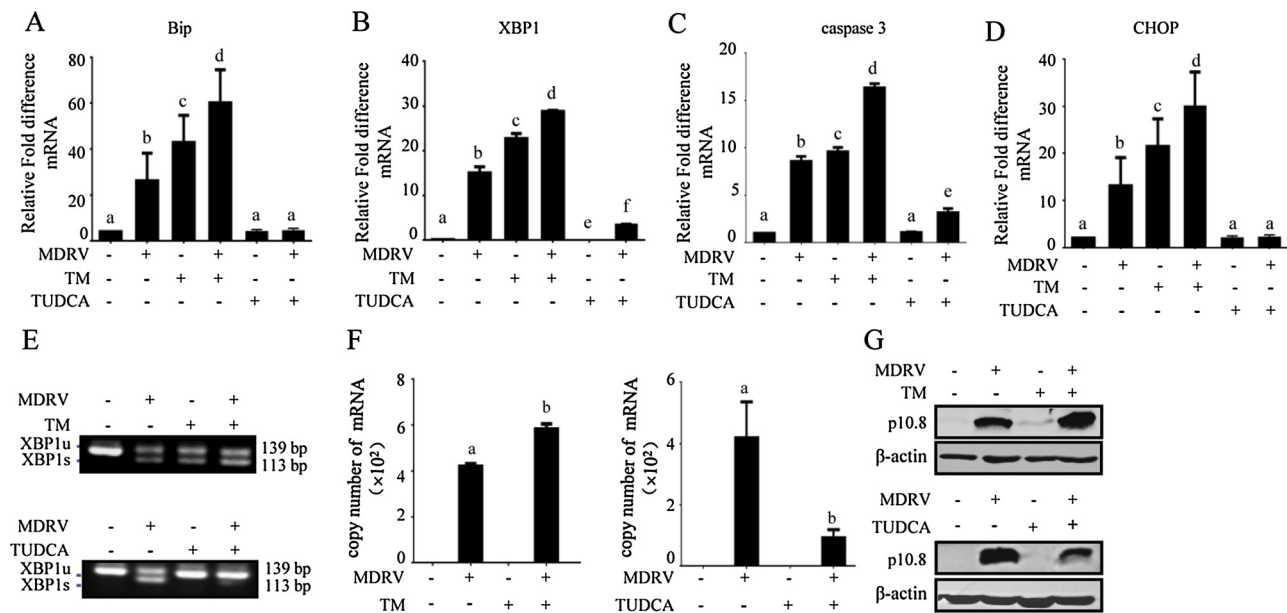


**Fig. 3.** Tunicamycin (TM) and Tauroursodeoxycholic acid (TUDCA) promoted or inhibited ER stress and apoptosis in MDRV-infected DF-1 cells. Six groups of DF-1 cells were cultured in a 6-well plate for 24 h. The first was the control; the second was infected with 0.2 mL of MDRV (0.01 TCID<sub>50</sub> = 10<sup>-5.40</sup>); the third was treated with TM (final concentration 1 mmol/L); the fourth was treated with 0.2 mL of MDRV (0.01 TCID<sub>50</sub> = 10<sup>-5.40</sup>) and TM; the fifth was treated with TUDCA (final concentration 1 mmol/L); the sixth was treated with 0.2 mL of MDRV (0.01 TCID<sub>50</sub> = 10<sup>-5.40</sup>) and TUDCA (final concentration 1 mmol/L) simultaneously. At 24 h post-infection, all cells in the six groups were collected. The mRNA levels of *Bip* (A), *XBP1* (B), *caspase 3* (C), and *CHOP* (D) were detected by RT and real time fq-PCR in all treatments. (E) The spliced *XBP1* level was detected by RT-PCR and PCR products were analyzed by DNA electrophoresis. (F–G) The mRNA and protein levels of p10.8 in MDRV-infected or mock-infected DF-1 cells treated with TM or TUDCA were analyzed by RT and real time fq-PCR and Western blots. All data represents mean ± SE of three independent experiments. Significance between the treatments was determined by One-Way ANOVA analysis and LSD test using SPSS software (Version 20.0). Means with different alphabets (a, b) denotes significance at  $p < 0.05$ .

these levels (Fig. 3F and G), suggesting that MDRV induces ER stress benefiting virus replication.

### 3.3. MDRVp10.8 protein induces apoptosis through ER stress in DF-1 cells

In the current study we investigate whether the p10.8 protein induces apoptosis through ER stress in DF-1 cells. First, our results reveal that at 24 h post-transfection, the MDRV p10.8 protein was detected (Fig. 4A). The mRNA level of *XBP1* was significantly increased compared with the control- and pCI-neo plasmid-transfected cells by RT and real time fq-PCR (Fig. 4B). Furthermore, we found that the MDRV p10.8 protein could promote the conversion of *XBP1u* to *XBP1s*, as revealed by DNA electrophoresis (Fig. 4C). We also found that the ER diameter of the p10.8-transfected cells was significantly wider than that in the controls and pCI-neo plasmid-transfected cells (Fig. 4D and E), suggesting that the MDRV p10.8 protein induces ER stress in DF-1 cells. Furthermore, we found that at the same time point, the apoptotic rate (%) were increased significantly in p10.8-transfected DF-1 cells compared with that in the control and pCI-neo plasmid-transfected cells (Fig. 4F and G). These results suggest that the MDRV p10.8 protein induces ER stress and apoptosis in DF-1 cells.

However, the question of whether p10.8-induced apoptosis via the ER stress still needs further investigation. The use of TM showed that the mRNA levels of *Bip* (Fig. 5A), *XBP1* (Fig. 5B), *caspase 3* (Fig. 5C), and *CHOP* (Fig. 5D) were significantly increased in p10.8-transfected DF-1 cells at 24 h post-transfection while the use of TUDCA reversed the MDRV p10.8-mediated increase in mRNA levels of *Bip* (Fig. 5A), *XBP1* (Fig. 5B), *caspase 3* (Fig. 5C) and *CHOP* (Fig. 5D). The increased levels of spliced *XBP1* were seen in p10.8-transfected or TM-treated DF-1 cells (Fig. 5E; upper panel). The elevated levels of spliced *XBP1* by the MDRV p10.8 were reversed in TUDCA-treated DF-1 cells (Fig. 5E; lower panel, lane 4). Furthermore, the percentage of apoptotic cells was also significantly reduced in p10.8-transfected DF-1 cells treated with TUDCA compared with that in similar untreated cells (Fig. 5F and G). In

addition, the apoptosis rate increased significantly in p10.8-transfected and TM-treated DF-1 cells (Fig. 5F and G). These results indicate that the MDRV p10.8 protein induced apoptosis through ER stress.

### 3.4. Knockdown of *XBP1* reduced ER stress and p10.8-induced apoptosis

To investigate the role of *XBP1s* in p10.8-mediated ER stress and -induced apoptosis in DF-1 cells, a siRNA was used to knock down *XBP1*. *XBP1* was effectively suppressed by the *XBP1*-specific siRNA (Fig. 6A). Results from fq-PCR analysis suggested that the mRNA levels of *Bip* (Fig. 6A), *XBP1* (Fig. 6B), *caspase 3* (Fig. 6C), and *CHOP* (Fig. 6D) increased in p10.8-transfected cells. The p10.8-modulated increase in mRNA levels of *XBP1*, *caspase 3*, and *CHOP* were reversed in si*XBP1*-treated cells (Fig. 6B–D). In addition, PCR results showed that depletion of *XBP1* reversed p10.8-modulated increase in levels of *XBP1s* (Fig. 6E), ER swelling (Fig. 6F) and apoptosis proportion (Fig. 6G and H). However, the mRNA level of *Bip* remained unchanged. Therefore, we proposed that the MDRV p10.8 protein induces apoptosis, and that this effect was associated with *XBP1*.

### 3.5. p10.8-induced apoptosis is associated with ER stress through the *Bip*/IRE1/*XBP1* pathway

To further confirm the molecular mechanism that p10.8-induced apoptosis is associated with ER stress through the *Bip*/IRE1/*XBP1* pathway, Western blot, Co-IP, and siRNA were used to evaluate the protein levels of *Bip*, p-IRE1, *XBP1s*, and cleaved *caspase 3*. Firstly, the increased levels of *Bip* was found in p10.8-transfected cells (Fig. 7A). Co-IP results indicated that the MDRV p10.8 protein disassociates the *Bip*/IRE1 complex (Fig. 7B). Western blot confirmed that p10.8-induced IRE1 phosphorylation (Fig. 8A) could enhance the conversion of *XBP1u* to *XBP1s* (Fig. 8A) and causes cleavage of pro-*caspase 3*, triggering apoptosis in transfected cells (Fig. 8A). Secondly, following treatment with the IRE1 inhibitor 4u8c, the p10.8-modulated increased levels of

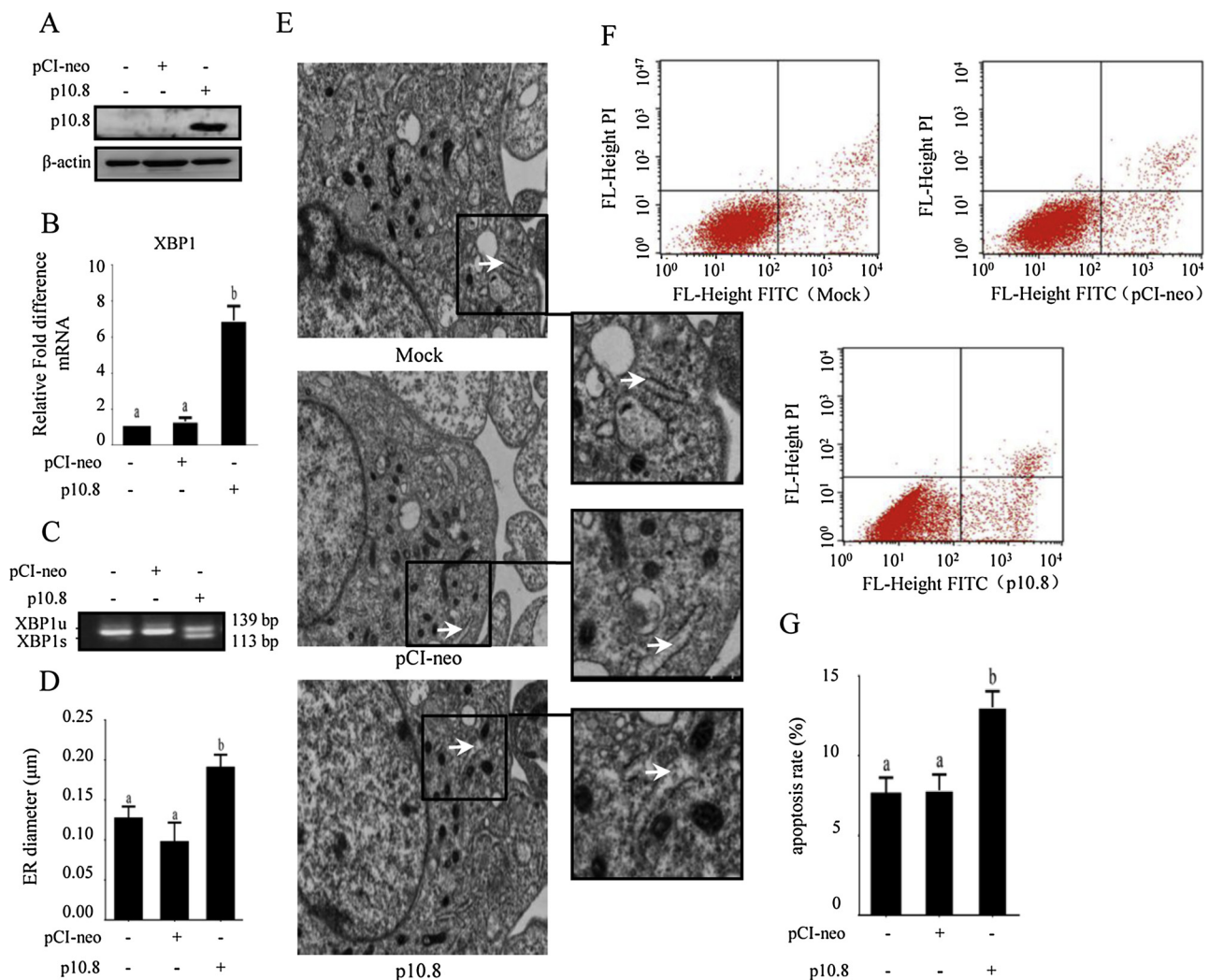


**Fig. 4.** The MDRV p10.8 protein induces ER stress and apoptosis in DF-1 cells. DF-1 cells were cultured in a 6-well plate for 24 h. Three groups of DF-1 cells were cultured in a 6-well plate for 24 h. The first was the control; the second was transfected with pCI-neo plasmid; and the third was transfected with pCI-neo-p10.8. At 24 h post-transfection, all cells in the three groups were collected. (A) MDRV was detected by Western blot assay with an anti-p10.8 antibody. The mRNA levels of *XBP1* (B) were detected by RT and real time fq-PCR. (C) The spliced *XBP1* level was detected by RT-PCR and PCR products were analyzed by DNA electrophoresis. (D, E) The ER diameter was determined by transmission electron microscope (HT7700, 8000 $\times$ , arrows indicating ER) and statistically analyzed. (F, G) Apoptosis in DF-1 cells was detected by flow cytometry and statistically analyzed (F). Statistical analysis of the proportions of cell apoptosis in p10.8-transfected DF-1 cells (G). All data represents mean  $\pm$  SE of three independent experiments. Significance between the treatments was determined by One-Way ANOVA analysis and LSD test using SPSS software (Version 20.0). Means with different alphabets (a, b) denotes significance at  $p < 0.05$ .

p-IRE1, XBP1s, and cleaved-caspase 3 were reversed (Fig. 8A). Furthermore, knockdown of XBP1 also showed that cleaved-caspase 3 was inhibited in p10.8-transfected cells (Fig. 8B). Collectively, our results reveal that p10.8-induced apoptosis is associated with ER stress through the Bip/IRE1/XBP1 pathway.

#### 4. Discussion

In the present study, we provide novel findings of the MDRV p10.8-mediated ER stress to induce apoptosis through the Bip/IRE1/XBP1 pathway in DF-1 cells and duckling hepatic tissues. We have previously showed that the MDRV p10.8 protein induces ER stress that causes cell cycle arrest and apoptosis through the PERK-eIF2 $\alpha$  pathway (Wang et al., 2018). In the current study, we further demonstrates that this viral protein induces apoptosis through ER stress employing another signaling pathway Bip/IRE1/XBP1. The current study would help to understand the mechanism of apoptosis-induced by MDRV. The ER is a crucial organelle involved in the synthesis, processing, and modification of proteins (Rayess et al., 2018). When proteins have been folded,

they are sent to the Golgi apparatus for modification and packaging. Unfolded proteins or defective folding proteins are then degraded in the ER (Ge et al., 2017). However, if these proteins are not degraded, but accumulated in the ER, they would cause ER stress. There are three transmembrane proteins PKR-like ER kinase (PERK), inositol-requiring enzyme 1 alpha (IRE1 $\alpha$ ), and activating transcription factor (ATF6) in endoplasmic reticulum. PERK and IRE1 $\alpha$  are the proximal effectors of endoplasmic reticulum stress (Wang et al., 2018). Serine/threonine protein kinase domain and RNase domain are found in IRE1 C-terminal, but only threonine protein kinase domain in PERK C-terminal. In the ER stress, the phosphorylated IRE1 $\alpha$  uses RNase domain to slice off an intron in mRNA of XBP1, which encodes a functional XBP1 protein (XBP1s). XBP1s enters into nucleus and regulates CHOP to induce host cell apoptosis (Huang et al., 2016). Phosphorylated PERK further causes phosphorylation of downstream protein eIF2 $\alpha$ , which inhibits protein biosynthesis, initiating the MDRV p10.8 protein to induce ER stress, resulting in apoptosis.

Viral infection is an important factor of influencing ER stress in cells (De Leo et al., 2017). Viral replication in host cells is regulated to cause

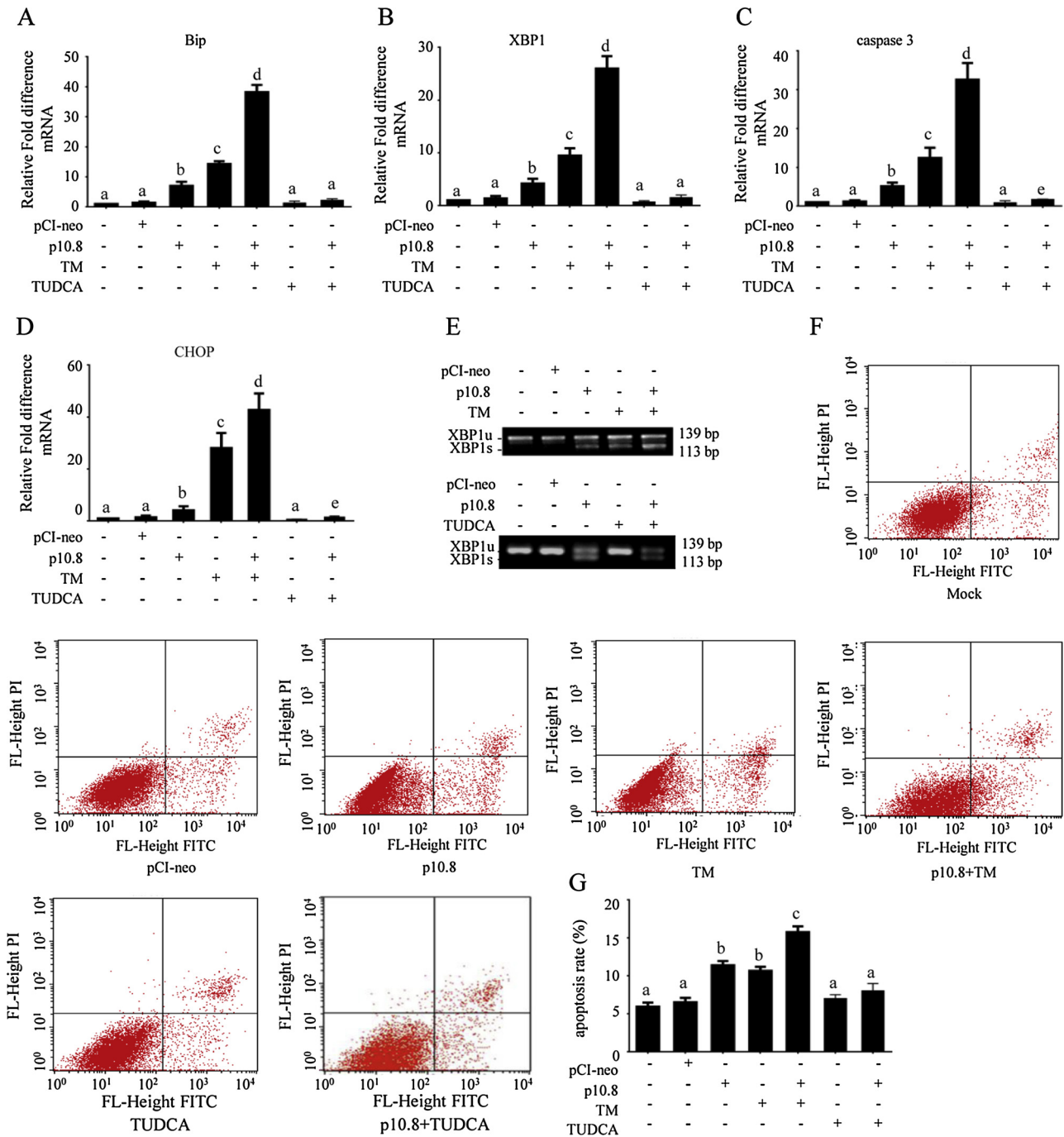


**Fig. 5.** Tunicamycin and Tauroursodeoxycholic acid promoted or inhibited MDRV-induce ER stress and apoptosis in p10.8-transfected DF-1 cells. Seven groups of DF-1 cells were cultured in a 6-well plate for 24 h. The first was the control; the second was transfected with pCI-neo plasmid; the third was transfected with pCI-neo-p10.8; the fourth was treated with TM (final concentration 1 mmol/L); and the fifth was transfected with pCI-neo-p10.8 for 6 h, followed by treatment of TM; the sixth was treated with TUDCA (final concentration 1 mmol/L); the seventh was transfected with pCI-neo-p10.8 and, after 6 h transfection, TUDCA was added into the DMEM medium. At 24 h post-transfection, all cells in the five groups were collected. The mRNA levels of *Bip* (A), *XBP1* (B), *caspase 3* (C), and *CHOP* (D) were determined by RT and real time q-PCR. (E) The spliced *XBP1* level was detected by RT-PCR and PCR products were analyzed by DNA electrophoresis. (F–G) Apoptosis in DF-1 was detected by flow cytometry and statistically analyzed (F). Statistical analysis of the proportions of cell apoptosis were analyzed (G). All data represents mean ± SE of three independent experiments. Significance between the treatments was determined by One-Way ANOVA analysis and LSD test using SPSS software (Version 20.0). Means with different alphabets (a, b) denotes significance at  $p < 0.05$ .

a large increase in unfolded or defectively folded polypeptides, which result in ER stress. Avian reovirus has been reported to up-regulate ER stress response proteins (Lin et al., 2015). Benali-Furet et al. reported that core constructs of Hepatitis C virus trigger hyper-expression of Grp78/Bip, Grp94, calreticulin, and sarco/endoplasmic reticulum calcium ATPase, inducing ER stress (Benali-Furet et al., 2005). Moreover,

bovine viral diarrhea virus activates the ER transmembrane kinase PERK (PKR-like ER kinase) and causes hyperphosphorylation of the translation initiation factor eIF2 alpha, consistent with the induction of an ER stress response (Jordan et al., 2002). In MDRV-infected five-day-old ducklings and DF-1 cells, Bip and XBP1 were activated, and we first confirms that MDRV induces ER stress in duckling liver tissues and DF-1

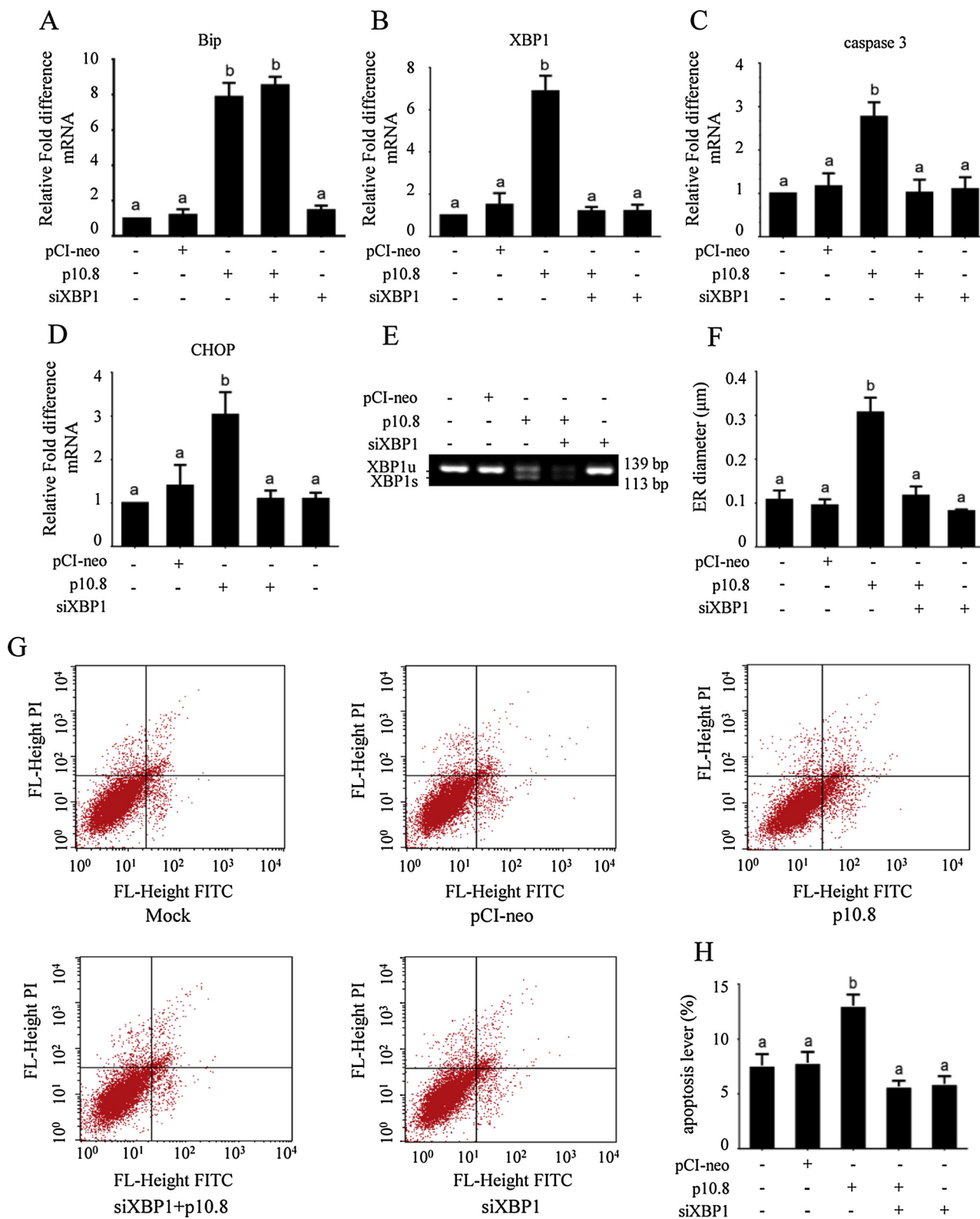


**Fig. 6.** Knockdown of XBP1 reduced p10.8 protein-induced ER stress and apoptosis. Five groups of DF-1 cells were cultured in a 6-well plate for 24 h. The first was the control; the second was transfected with pCI-neo plasmid; the third was transfected with pCI-neo-p10.8; the fourth was transfected with XBP1 siRNA followed with 6 h transfection with pCI-neo-p10.8; and the fifth was transfected with siXBP1. At 24 h post-transfection pCI-neo-p10.8, all cells in the five treatments were collected. The mRNA levels of *Bip* (A), *XBP1* (B), *caspase 3* (C), and *CHOP* (D) was determined by RT and real time fq-PCR. (E) The spliced *XBP1* level was detected by RT-PCR and PCR products were analyzed by DNA electrophoresis. (F) ER diameter was objected by transmission electron microscope objection (HT7700, 8000×) and statistically analyzed. (G, H) Apoptosis in DF-1 cells was detected by flow cytometry and statistically analyzed (G). Statistical analysis of the proportions of cell apoptosis in DF-1 cells were analyzed (G). All data represents mean ± SE of three independent experiments. Significance between the treatments was determined by Student's t-test using SPSS software (Version 20.0). Means with different alphabets (a, b) denotes significance at p < 0.05.

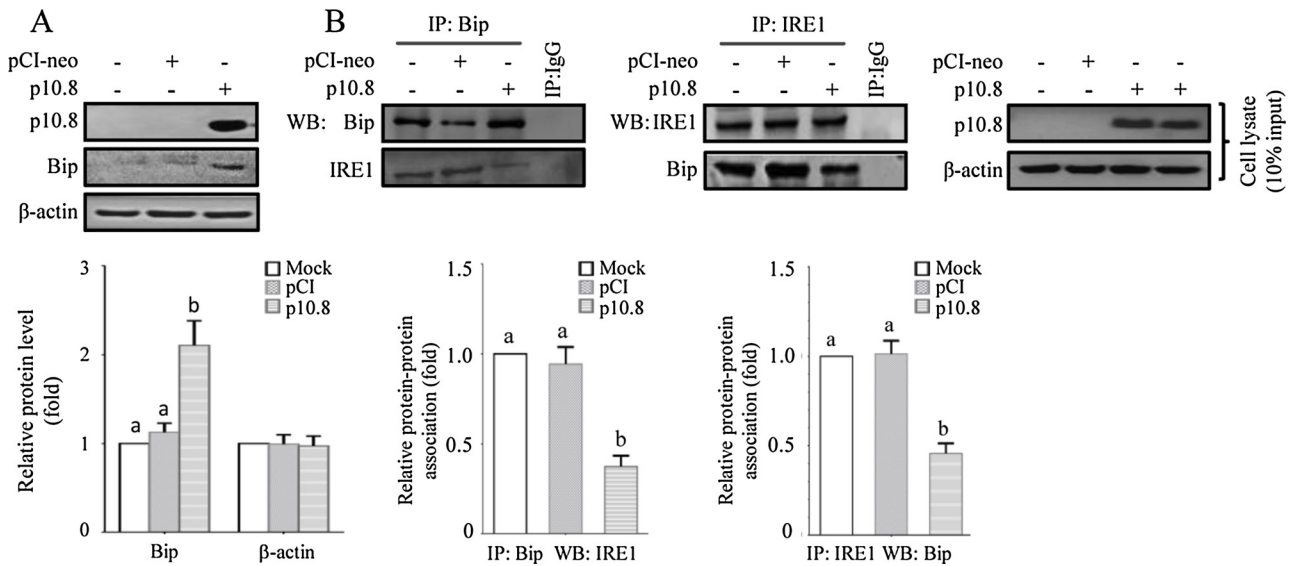


**Fig. 7.** p10.8 protein promotes disassociation of the Bip/IRE1 complex. At 24 h post the transfection of pCI-neo-p10.8 in DF-1 cells, (A) Bip protein expression in three groups of DF-1 cells (mock, pCI-neo, and p10.8) was analyzed by Western blot assays using β-actin as the reference protein. Relative protein expression levels were measured and statistically analyzed. (B) In reciprocal co-immunoprecipitation experiments, the binding of BIP and IRE1 was examined in p10.8-transfected DF-1 cells at 24 h post-transfection. Western blot analysis of BIP and IRE1 contained in BIP or IRE1 immunoprecipitates was performed. Signals in all Western blots were quantified with Image J software. The amounts of BIP /IRE1 association were normalized against the value in the negative control. The levels of the negative control was considered 1-fold. All data represents mean ± SE of three independent experiments. Significance between the treatments was determined by One-Way ANOVA analysis and LSD test using SPSS software (Version 20.0). Means with different alphabets (a, b) denotes significance at p < 0.05.

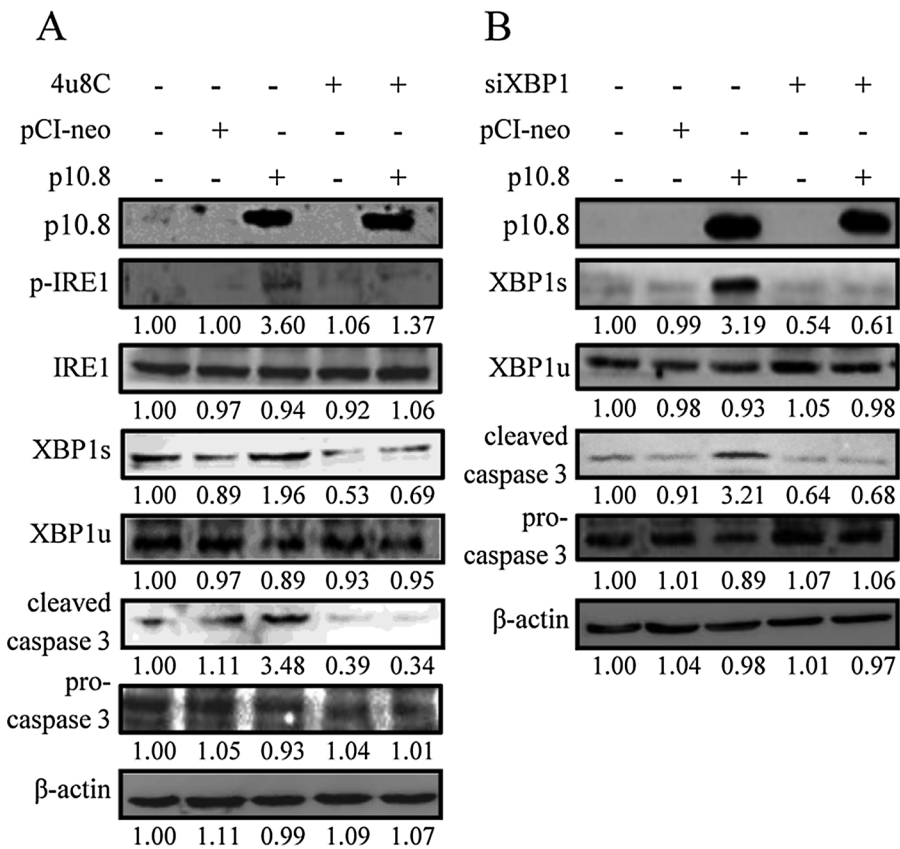


**Fig. 8.** p10.8 protein promotes the activation of IRE1, XBP1 and caspase 3. (A) The IRE1 inhibitor 4u8c (final concentration 1 mmol/L) was used. At 24 h post transfection, p10.8, Bip, IRE1, p-IRE1, XBP1u, XBP1s, pro-caspase 3, and cleaved-caspase 3 in five groups of DF-1 cells (mock, pCI-neo, 4u8c and 4u8c + p10.8) were analyzed by Western blot. (B) XBP1 siRNA was used to knockdown XBP1, the levels of p10.8, Bip, IRE1, p-IRE1, XBP1u, XBP1s, pro-caspase 3, and cleaved-caspase 3 were analyzed by Western blot. β-actin was used as a loading control.

cells. When ER stress occurs in a cell, the unfolded protein response (UPR) may be used to adapt and adjust the synthesis of new proteins. However, long-time overload of ER stress would induce apoptosis to remove the damaged cells.

Many reports have demonstrated that viruses cause ER stress-induced apoptosis. Some studies have demonstrated the Bip/GRP79 up

regulation participates in apoptosis induction (Lin et al., 2015; Mukherjee et al., 2017; Wang et al., 2018). It was reported that the structural protein sigma C of ARV is an apoptosis inducer (Shih et al., 2004). Lin et al. proposed that ARV-induced apoptosis was associated with p53 and mitochondrial pathway (Chulu et al., 2007) and Bip/GRP79-mediated Bim translocation to the ER (Lin et al., 2015).

Mukherjee et al. found that Japanese encephalitis virus induces human neural stem/progenitor cell death by elevating GRP78, PHB, and hnRNP through ER stress (Mukherjee et al., 2017). In our previous study, we have demonstrated that MDRV induces apoptosis through multiple signaling pathways, as revealed by transcriptomic analysis (Wang et al., 2017a). The current study further confirms that MDRV induces ER stress as well as apoptosis in duckling hepatic and DF-1 cells. Using TM and TUDCA, we confirmed that MDRV-induced apoptosis is associated with the ER stress. Viral infection is one of the important stimulants of cell apoptosis (Boehme et al., 2013), as viruses must complete DNA replication before the infected cells become necrotic (Neumann et al., 2015). Sometimes viruses utilize host cell apoptosis to accelerate viral replication and assembly (Kucharski et al., 2016). In this study, we found that MDRV-induced ER stress-associated apoptosis is beneficial for MDRV replication.

Virus-induced apoptosis is usually accomplished by one or more viral proteins. Porcine circovirus type 2 capsid protein induces an unfolded protein response with subsequent activation of apoptosis (Zhou et al., 2017). Hepatitis B virus X protein inhibits apoptosis by modulating the ER stress response (Li et al., 2017). MDRV infection outbreaks in China have caused serious damage to duckling farms since 1997 (Wu et al., 2001; Wang et al., 2015). The current study reveals that the MDRV p10.8 protein induces apoptosis through ER stress, which is an important supplement to the pathogenic mechanism of MDRV infection in duckling liver.

In order to elucidate the molecular mechanism underlying p10.8-induced apoptosis through ER stress, we investigated whether the Bip/IRE1/XBP1 pathway plays a role in p10.8-induced apoptosis. Bip is the molecular chaperone of ER stress. Under normal conditions, Bip binds to IRE1 and inhibits its activation. Our findings clearly demonstrate the MDRV p10.8 elicits XBP1 activity by disassociating the Bip/IRE1 complex, suggesting that the p10.8 act on XBP1 splicing. The MDRV p10.8 protein disassociates the Bip/IRE1 complex and increases the phosphorylated form of IRE1 to activate XBP1. Our findings reveal that MDRV p10.8-induced apoptosis is associated with ER stress through the Bip/IRE1/XBP1 pathway.

## 5. Conclusion

The findings in this study first reveal the induction of ER stress by MDRV in duckling liver and DF-1 cells. We demonstrated that the MDRV p10.8 protein is the major protein to up-regulate ER stress which induces apoptosis through the Bip/IRE1/XBP1 pathway.

## Acknowledgements

This work was supported by grants from the China National Natural Science Foundation (No.31372474), the Promote Both Sides of the Taiwan Straits Science and Technology Cooperation Foundation (No. U1305212), the iEGG and Animal Biotechnology Center from the Feature Areas Research Center Program within the framework of the Higher Education Sprout Project by the Ministry of Education (MOE) in Taiwan the Ministry of Science (MOE-107-S-0023-B), and the Ministry of Science and Technology of Taiwan (MOST 106-2313-B-005-054-MY3).

## References

Ahronian, L.G., Lewis, B.C., 2014. Generation of high-titer RCAS virus from DF-1 chicken fibroblasts. *Cold Spring Harb. Protoc.* 11, 1161–1166.

Amin-Wetzel, N., Saunders, R.A., Kamphuis, M.J., Rato, C., Preissler, S., Harding, H.P., Ron, D., 2017. A J-protein co-chaperone recruits Bip to monomerize IRE1 and repress the unfolded protein response. *Cell* 171, 1625–1637.

Benali-Furet, N.L., Chami, M., Houel, L., De Giorgi, F., Vernejoul, F., Lagorce, D., Buscail, L., Bartenschlager, R., Ichas, F., Rizzuto, R., Paterlini-Brechot, P., 2005. Hepatitis C virus core triggers apoptosis in liver cells by inducing ER stress and ER calcium depletion. *Oncogene* 24, 4921–4933.

Boehme, K.W., Hammer, K., Tollefson, W.C., Konopka-Anstadt, J.L., Kobayashi, T.,

Dermody, T.S., 2013. Dermody nonstructural protein  $\sigma$ 1s mediates reovirus-induced cell cycle arrest and apoptosis. *J. Virol.* 87, 12967–12979.

Cai, Y., Zhuang, Y., Zhou, W., Wu, B., Qiu, X., Wang, Q., 2015. Cloning, sequence analysis and predicted protein construction of MDRV p10 gene. *J. Fujian Agric. Forestry Univ. (Nat. Sci. Ed.)* 44, 606–611.

Cao, Y., Hao, Y., Li, H., Liu, Q., Gao, F., Liu, W., Duan, H., 2014. Role of endoplasmic reticulum stress in apoptosis of differentiated mouse podocytes induced by high glucose. *Int. J. Mol. Med.* 33, 809–816.

Chen, Z., Luo, G., Wang, Q., Wang, S., Chi, X., Huang, Y., Wei, H., Wu, B., Huang, S., Chen, J.L., 2015. Muscovy duck reovirus infection rapidly activates host innate immune signaling and induces an effective antiviral immune response involving critical interferons. *Vet. Microbiol.* 175, 232–243.

Chulu, J.L., Lee, L.H., Lee, Y.C., Liao, S.H., Lin, F.L., Shih, W.L., Liu, H.J., 2007. Apoptosis induction by avian reovirus through p53 and mitochondria-mediated pathway. *Biochem. Biophys. Res. Commun.* 356, 529–535.

De Leo, A., Chen, H.S., Hu, C.A., Lieberman, P.M., 2017. Deregulation of KSHV latency conformation by ER-stress and caspase-dependent RAD21-cleavage. *PLoS Pathog.* 13 (8), e1006596.

Gaudry, D., Charles, J.M., Tektoff, J., 1972. A new disease expressing itself by a viral pericarditis in Barbary ducks. *C. R. Acad. Sci. Hebd. Seances Acad. Sci. D* 274, 2916–2919.

Ge, M., Luo, Z., Qiao, Z., Zhou, Y., Cheng, X., Geng, Q., Cai, Y., Wan, P., Xiong, Y., Liu, F., Wu, K., Liu, Y., Wu, J., 2017. HERP binds TBK1 to activate innate immunity and repress virus replication in response to endoplasmic reticulum stress. *J. Immunol.* 199 (9), 3280–3292.

Geng, H., Zhang, Y., Liu, P.Y., Vanhanseng, G.D., Wang, Y., Liu, M., Tong, G., 2009. Apoptosis p10.8 protein in primary duck embryonated fibroblast and Vero E6 cells. *Avian Dis.* 53, 434–440.

Gu, Y.H., Wang, Y., Bai, Y., Liu, M., Wang, H.L., 2017. Endoplasmic reticulum stress and apoptosis via PERK-eIF2 $\alpha$ -CHOP signaling in the methamphetamine-induced chronic pulmonary injury. *Environ. Toxicol. Pharmacol.* 49, 194–201.

Guo, D., Qiu, N., Shaozhou, W., Bai, X., He, Y., Zhang, Q., Zhao, J., Liu, M., Zhang, Y., 2014. Muscovy duck reovirus p10.8 protein localizes to the nucleus via a non-conventional nuclear localization signal. *Virol. J.* 11, 37.

Huang, M., Xu, A., Wu, X., Zhang, Y., Guo, Y., Guo, F., Pan, Z., Kong, L., 2016. Japanese encephalitis virus induces apoptosis by the IRE1/JNK pathway of ER stress response in BHK-21 cells. *Arch. Virol.* 161, 699–703.

Jiang, Q., Chen, J., Liu, S., Liu, G., Yao, K., Yin, Y., 2017. Glutamine attenuates apoptosis induced by endoplasmic reticulum stress by activating the IRE1 $\alpha$ -XBP1 axis in IPEC-J2: a novel mechanism of l-glutamine in promoting intestinal health. *Int. J. Mol. Sci.* 18 pii: E2617.

Jordan, R., Wang, L., Graczyk, T.M., Block, T.M., Romano, P.R., 2002. Replication of a cytopathic strain of bovine viral diarrhea virus activates PERK and induces endoplasmic reticulum stress-mediated apoptosis of MDBK cells. *J. Virol.* 76, 9588–9599.

Kaschula, V.R., 1950. A new virus disease of the Muscovy duck (*Cairina moschata* Linn.) Present in Natal. *J. S. Afr. Vet. Med. Assoc.* 21, 19–26.

Ke, G.M., Cheng, H.L., Ke, L.Y., Ji, W.T., Chulu, J.L.C., Liao, M.H., Chang, T.J., Liu, H.J., 2006. Development of a quantitative light cycler real-time RT-PCR for detection of avian reovirus. *J. Virol. Methods* 133, 6–13.

Kucharski, T.J., Ng, T.F., Sharon, D.M., Navid-Azarbaijani, P., Tavassoli, M., Teodoro, J.G., 2016. Activation of the chicken anemia virus apoptin protein by Chk1/2 phosphorylation is required for apoptotic activity and efficient viral replication. *J. Virol.* 90, 9433–9445.

Li, J., He, J., Fu, Y., Hu, X., Sun, L.Q., Huang, Y., Fan, X., 2017. Hepatitis B virus X protein inhibits apoptosis by modulating endoplasmic reticulum stress response. *Oncotarget* 8, 96027–96034.

Lin, P.Y., Liu, H.J., Chang, C.D., Chen, Y.C., Chang, C.I., Shih, W.L., 2015. Avian reovirus S1133-induced apoptosis is associated with Bip/GRP79-mediated Bim translocation to the endoplasmic reticulum. *Apoptosis* 20, 481–490.

Liu, H.J., Lin, P.Y., Wang, L.R., Hsu, H.Y., Liao, M.H., Shih, W.L., 2008. Activation of small GTPases RhoA and Rac1 is required for avian reovirus p10-induced syncytium formation. *Mol. Cells.* 26, 396–403.

Mukherjee, S., Singh, N., Sengupta, N., Fatima, M., Seth, P., Mahadevan, A., Shankar, S.K., Bhattacharyya, A., Basu, A., 2017. Japanese encephalitis virus induces human neural stem/progenitor cell death by elevating GRP78, PHB and hnRNPC through ER stress. *Cell Death Dis.* 8, e2556.

Neumann, S., El Maadidi, S., Faletti, L., Haun, F., Labib, S., Schejtmann, A., Maurer, U., Borner, C., 2015. How do viruses control mitochondria-mediated apoptosis? *Virus Res.* 209, 45–55.

Rayess, H.M., Xi, Y., Garshott, D.M., Brownell, A.L., Yoo, G.H., Callaghan, M.U., Fribley, A.M., 2018. Benzethonium chloride activates ER stress and reduces proliferation in HNSCC. *Oral Oncol.* 76, 27–33.

Shah, A., Vaidya, N.K., Bhat, H.K., Kumar, A., 2016. HIV-1 gp120 induces type-1 programmed cell death through ER stress employing IRE1 $\alpha$ , JNK and AP-1 pathway. *Sci. Rep.* 6, 18929.

Shih, W.L., Hsiao, H.W., Liao, M.H., Lee, L.H., Liu, H.J., 2004. Avian reovirus  $\sigma$ C protein induces apoptosis in cultured cells. *Virology* 321, 65–74.

Taylor, R.C., Dillin, A., 2013. XBP-1 is a cell-nonautonomous regulator of stress resistance and longevity. *Cell* 153, 1435–1447.

Wang, Q.X., Wu, Y.J., Cai, Y.L., Zhuang, Y.B., Xu, L.H., Wu, B.C., Zhang, Y.D., 2015. Spleen transcriptome profile of Muscovy ducklings in response to infection with Muscovy duck reovirus. *Avian Dis.* 59, 282–290.

Wang, Q.X., Liu, M.X., Chen, S.Y., Wu, Y.J., Zhuang, Y.B., Li, C.Y., Huang, Y.F., Wu, B.C., 2017a. Transcriptomic analysis reveals the molecular mechanism of apoptosis induced by Muscovy duck reovirus. *Genes Genom.* 39, 1227–1235.

- Wang, Q.X., Liu, M.X., Xu, L.H., Zhou, W.D., Wu, Y.J., Huang, Y.F., 2017b. Transcriptome analysis reveals the molecular mechanism of hepatic fat metabolism disorder caused by Muscovy duck reovirus infection. *Avian Pathol.* 47, 127–139.
- Wang, Q.X., Yuan, X.Q., Chen, Y., Zheng, Q.L., Xu, L.H., Wu, Y.J., 2018. Endoplasmic reticulum stress mediated MDRV p10.8 protein-induced cell cycle arrest and apoptosis through PERK/eIF2 $\alpha$  pathway. *Front. Microbiol.* 9, 132721.
- Wu, B.C., Chen, J.X., Yao, J.S., 2001. Isolation and identification of Muscovy duck reovirus. *J. Fujian Agric. Forestry Univ. (Nat. Sci. Ed.)* 3, 227–230.
- Zhang, X., Tang, S., Zhang, Q., Shao, W., Han, X., Wang, Y., Du, Y., 2016. Endoplasmic reticulum stress mediates JNK-dependent IRS-1 serine phosphorylation and results in Tau hyperphosphorylation in amyloid  $\beta$  oligomer-treated PC12 cells and primary neurons. *Gene* 587, 183–193.
- Zhou, Y.S., Gu, Y.X., Qi, B.Z., Zhang, Y.K., Li, X.L., Fang, W.H., 2017. Porcine circovirus type 2 capsid protein induces unfolded protein response with subsequent activation of apoptosis. *J. Zhejiang Univ. Sci. B* 18, 316–323.